Electron cyclotron emission imaging diagnostic system for Rijnhuizen Tokamak Project

B. H. Deng, R. P. Hsia, C. W. Domier, S. R. Burns, T. R. Hillyer, and N. C. Luhmann, Jr.
University of California at Davis, 228 Walker Hall, Davis, California 95616

T. Oyevaar, A. J. H. Donné, and the RTP team
FOM-Inst. voor Plasmafysica Rijnhuizen, Association Euratom-FOM

(Presented on 10 June 1998)

A 16-channel electron cyclotron emission (ECE) imaging diagnostic system has been developed and installed on the Rijnhuizen Tokamak Project for measuring plasma electron cyclotron emission with a temporal resolution of 2 μs. The high spatial resolution of the system is achieved by utilizing a low cost linear mixer/receiver array. Unlike conventional ECE diagnostics, the sample volumes of the ECE imaging system are aligned vertically, and can be shifted across the plasma cross-section by varying the local oscillator frequency, making possible 2D measurements of electron temperature profiles and fluctuations. The poloidal/radial wavenumber spectra and correlation lengths of T_e fluctuations in the plasma core can also be obtained by properly positioning the focal plane of the imaging system. Due to these unique features, ECE imaging is an ideal tool for plasma transport study. Technical details of the system are described, together with preliminary experimental results.
 [S0034-6748(99)69701-5]

I. INTRODUCTION

Electron cyclotron emission (ECE) radiometers have been standard diagnostics for measuring plasma electron temperature profiles in tokamaks since 1974.[1] In an optically thick plasma, the ECE power received by an antenna is proportional to the electron temperature. As the ECE frequency in a tokamak depends on magnetic field, which is a monotonically decreasing function of major radius, local T_e values can be obtained by frequency-resolved ECE measurements. Conventional ECE diagnostics measure electron temperature profiles by using a single antenna/receiver aligned along a horizontal chord in the direction of the major radius; therefore, 2D measurements are impossible with this single sight line setup. The spatial resolution of such a system in the transverse direction of the sight line is limited by the divergence of the beam pattern of the antenna, typically about 2–3 cm for small tokamaks.

Small scale structures (~1 cm) like filamentation and transport barriers are observed during high power electron cyclotron resonance heating (ECRH) on the Rijnhuizen Tokamak Project (RTP).[2,3] Therefore, high spatial resolution is essential for detailed investigations of these structures, which may lead to better understanding of plasma transport phenomena. On the other hand, microscopic plasma fluctuations are believed to be the cause of anomalous transport, an issue that is not resolved due to limits in fluctuation diagnostics, especially in the plasma core.[4] Recently, correlation techniques have been applied to ECE diagnostics to measure core electron temperature fluctuations.[5] To reveal the role of fluctuations in anomalous transport, it is desirable to have 2D measurements of the turbulent fluctuations as well as information regarding fluctuation wave numbers and correlation lengths. However, this is beyond the capability of conventional ECE diagnostics. Thus, the development of an ECE imaging (ECEI) diagnostic is motivated.

ECEI is a novel diagnostic system, in which high spatial resolution (~1 cm) is achieved by using a compact planar mixer/receiver array.[6] Unlike conventional ECE diagnostics, the sample volumes of the ECEI system are aligned vertically, with the horizontal position along the major radius defined by the magnetic field and the local oscillator (LO) frequency. With this setup, 2D measurements are obtained by varying the LO frequency and/or the magnetic field. Poloidal/radial wave numbers and correlation lengths of T_e fluctuations can be measured by properly positioning the vertically aligned focal plane of the imaging system.

The prototype ECEI system was developed and tested on the Texas Experimental Tokamak Upgrade (TEXT-U),[6] and has demonstrated its unique capability, especially in T_e fluctuation measurements.[7] In this article, we describe a 16-channel ECE imaging diagnostic system for RTP. With the improved mixer array design, and the use of a broadband high power backward wave oscillator (BWO) as the LO source, the system noise temperature is reduced by about an order of magnitude. Although the distance between the vacuum chamber and the imaging lenses is slightly larger than that of the prototype system due to the port accessibility, a similar spatial resolution (~1 cm) is achieved utilizing slightly larger lenses. With the fabrication and implementation of a 32-channel low noise, low cross-talk intermediate frequency (IF) signal processing electronic system, it is possible to simultaneously perform autocorrelation and cross-correlation measurements. Implementation of a dichroic plate filter permits the system to operate in 110 GHz ECRH discharges in the presence of strong stray radiation. In Sec. II, the experimental configuration and the system components including the mixer/receiver array, the imaging optics,

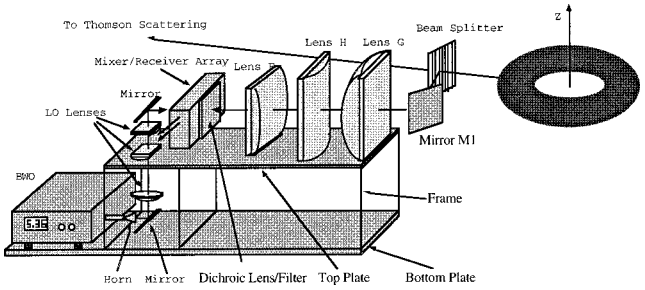

FIG. 1. Experimental configuration of the RTP ECE imaging diagnostic system, consisting of the imaging optics, the mixer/receiver array, the local oscillator and power coupling optics, and two boxes of IF signal processing electronics which are omitted for clarity. The three LO lenses and lenses F, H, and G are made of HDPE. The bottom plate is the moving part of a motorized translation stage.

the LO and coupling optics, the support frame, the IF signal processing electronics, and the millimeter wave shielding are discussed in detail. Experimental measurements of plasma electron temperature profiles and fluctuations in RTP are presented in Sec. III.

II. THE SYSTEM DESCRIPTION

A. Experimental configuration

Shown in Fig. 1 is the experimental configuration of the RTP ECEI diagnostic system. It measures the second harmonic, extraordinary mode electron cyclotron radiation (100–140 GHz) of the plasma from the same horizontal port as the Thomson scattering system; therefore, a direct comparison between the two systems is possible. Another advantage of this arrangement is that the Thomson scattering system provides a very convenient calibration method for the ECEI system. This can be done for each plasma discharge, thereby solving the problem of sensitivity variations with the local oscillator frequency. The beam splitter is comprised of tungsten wires of 10 μm in diameter that are stretched vertically on a metal frame 46 cm high by 26 cm wide (clear aperture), with an interwire spacing of 150 μm. It has a reflection coefficient greater than 98% in the frequency range of interest, while causing negligible distortion of the Thomson scattering signals. An aluminum turning mirror (M1) then reflects the ECE radiation away from the transformer yoke of the tokamak. This setup yields a minimum distance of about 120 cm between the center of the vacuum chamber and the front side of lens G. Other than the beam splitter and the turning mirror (M1), all other system components and corresponding support structures are mounted on a motorized translation stage which can translate the system horizontally by greater than 30 cm. The translation stage makes it possible to keep a tight focusing at the plasma resonant layer from $r=-10$ cm (high field side) to $r>a$, where $a=16.5$ cm is the minor radius of RTP. Omitted in Fig. 1 are two shielding boxes for the IF signal processing electronics, which are attached to the support frame near the mixer/receiver array.

B. Mixer/receiver array

The mixer/receiver array is comprised of planar slot bow tie (SBT) antennas integrated with T/O Device beam-lead Schottky diodes,[6] and has the advantages of wide radio frequency (rf) and intermediate frequency (IF) bandwidths, ease of fabrication, and low cost. A high density polyethylene (HDPE) hyperhemispheric lens is attached to the substrate side of the array, facing the plasma. The elements of the array are aligned along the **E** field (vertical) direction. The antenna pattern of the array is chosen as a compromise of optical design (Sec. II C). As the radiation is concentrated in the main lobe, the crosstalk between channels is very small. This is a very important advantage of the array, especially for fluctuation measurements (Sec. III).

C. Imaging optics

The beam splitter, the turning mirror M1, lenses G, H, and F, the dichroic lens, and the substrate lens attached to the array comprise the imaging optics. An array of sample volumes in the plasma, aligned along the vertical (z) direction (Fig. 1), is imaged onto the array. Ray tracing codes have been compiled to set up a one to one relation between the array elements and their images by choosing appropriate lens positions and focal lengths, have been utilized to design the lenses and to calculate the focal plane spot sizes. The goal of the optical design is to achieve the highest possible spatial resolution, consistent with conditions such as port access, reasonable lens sizes, and lens fabrication cost, etc. Generally, high spatial resolution requires that the focal plane spot size and the channel spacing be as small as possible. Given the optical magnification, which determines the channel spacing, a wider **E** Plane antenna pattern yields a smaller beam spot size. However, a smaller spot size results in more rapid beam divergence, which is limited by the port access and the sizes/cost of the imaging lenses. As a compromise, the 3 dB full width of the antenna pattern is chosen to be 15°.

The system was tested in situ after the installation, using millimeter waves scattered from an aluminum rod to simulate the ECE radiation. The focal plane location of the imaging optics is determined by translating the system to obtain

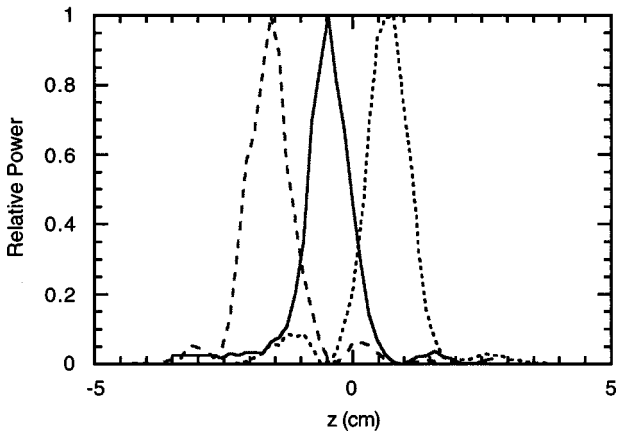

FIG. 2. Focal plane beam patterns measured at 115 GHz for the middle channels.

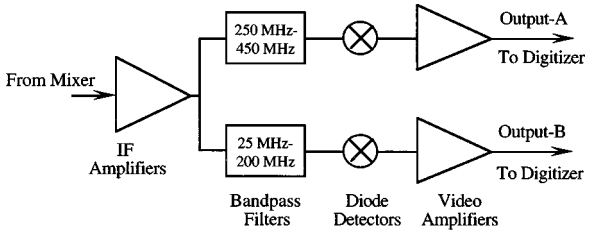

FIG. 3. Block diagram of one of the 16-channel IF signal detection circuits. The detector diodes and video amplifiers after the bandpass filters are integrated into compact IF detectors, which include the low pass video filters and current buffers to drive the 50 Ω input of the ADCs.

the narrowest beam pattern. By scanning the rod vertically, the focal plane beam pattern, the spot sizes, and the channel positions are obtained. Shown in Fig. 2 are the measured focal plane beam patterns for channels 6, 7, and 8. For all 16 channels, the average interchannel spacing is 1.3 ± 0.1 cm, which is the same value as predicted from the optical design. The beam waist $1/e$ intensity diameter is about 1 cm for the middle channels, which is very close to the designed value of 0.9 cm. This value increases to about 1.3 cm for the edge channels due to spherical aberrations and edge diffraction.

D. Local oscillator and power coupling optics

A broadband BWO is utilized as the local oscillator. This BWO is made by ELVA-1. It has a frequency range of 80–140 GHz, thus covering the whole frequency range of the second harmonic ECE in RTP. The BWO is well calibrated, easy to operate, and has a -30 dB radiation bandwidth within ±3 MHz and an output power that varies from ~40 mW at 80 GHz to ~200 mW at 120 GHz. The output of the BWO is coupled to the mixer array by two cylindrical lenses and one spherical lens comprised of HDPE, and two planar mirrors. The three HDPE lenses transform the output from an *F*-band horn antenna to an elliptical beam, focused at the mixer array. The mirrors in this LO setup are used to avoid interference with the tangential Thomson scattering system.

E. IF signal processing electronics and shielding

Shown in Fig. 3 is the block diagram of one of the 16-channel IF detection circuits. Each signal from the array mixer is preamplified (~45 dB) by MiniCircuits' low noise amplifiers, and split into ''A'' and ''B'' channels via SMA-Tees. The ''A'' and ''B'' channels are defined by two bandpass filters with nonoverlapping bandwidths. By applying correlation techniques to signals from ''A'' and ''B'' channels, it is possible to measure T_e fluctuations within the sample volume of a single imaging channel, while information such as the wave numbers and correlation lengths of T_e fluctuations is obtained from correlations between signals from different imaging channels.

The IF signals after the bandpass filters are converted into video signals by Metelics Corporation's MSS20000 series zero bias Schottky detector diodes. The diode detectors, video amplifiers, and low pass filters are integrated into compact, low cost IF detectors that are enclosed in shielding

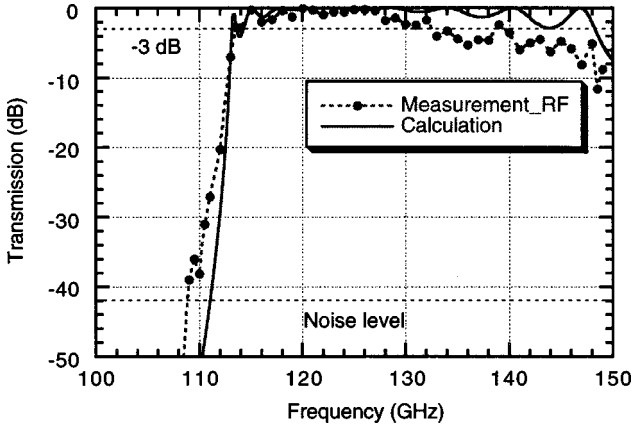

FIG. 4. Performance of the dichroic filter for shielding the 110 GHz ECRH stray radiation.-

boxes approximately $7.5\times6.5\times4$ cm^3 in size. The output voltage of the IF detectors is designed to be proportional to the input IF signal power (and thus proportional to T_e), and to match the ADC's 50 Ω input impedance and dynamic range of 0–1 V. The 3 dB frequency of the low pass filters is set to 250 kHz, with the possibility for it to be extended to 1 MHz. A total of 32 IF detectors are fabricated for the 16 mixer channels. The IF frequency response, sensitivity, and video response of the 32 IF detectors have been tested and the maximum variation between channels is within 10%.

A total of 16 channels of the circuit shown in Fig. 3 are shielded in two separate IF boxes, as mentioned in Sec. II A. The overall performance of the IF circuits have been tested in the laboratory, and the maximum difference between channels is about 3 dB, arising mainly from the variation in the gain (~45 dB total) of the preamplifiers. The crosstalk between any two channels is less than -60 dB.

In RTP, the stray radiation due to the 500 kW, 110 GHz ECRH system can reach a level of ~5 mW/cm^2. This power density can damage the array when it is focused by the imaging optics with a receiving area of about 61×28 cm^2 (lens G). Thus, good shielding is required. First, all the optical components attached to the translation stage (Fig. 1), from the horn antenna to lens G, are shielded in a shielding box built on site with aluminum plates. Eccosorb panels are glued to the aluminum plates at the inner side facing the optics to absorb stray radiation leaking into the box. As the flat side of lens G is left open to receive plasma radiation, a roof plate projects out from above lens G to the top of the turning mirror (M1), to reduce the incident stray radiation through this open area. However, most of the unabsorbed ECRH power coming through the port can still reach the array. This is rejected by the dichroic filter, which is attached to the cover plate of the mixer array (Fig. 1).

The dichroic filter is simply a perforated aluminum plate, with carefully chosen hole size and thickness to obtain the desired performance. As shown in Fig. 4, the measured performance is quite close to the theoretical predictions,[8] except at high frequencies where extra power loss arises due to the finite relative open area. The measured attenuation of 37 dB at 110 GHz turns out to be sufficient to protect the system

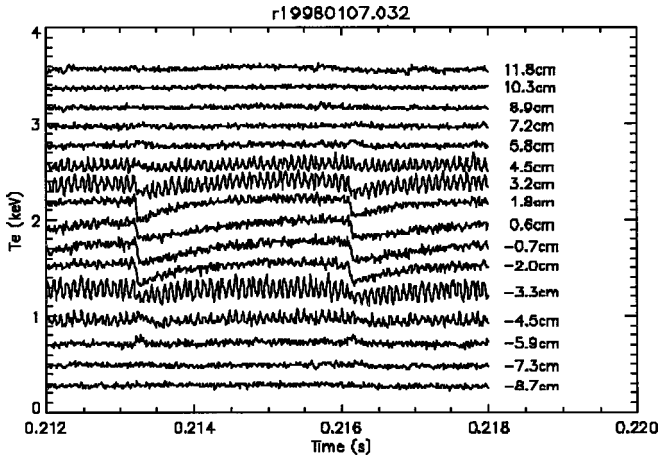

FIG. 5. Time traces of the ECEI signals during ECRH. The corresponding channel positions are denoted at the right column. A $m=2$ mode is observed to be localized at the sawtooth inversion radius. This figure demonstrate the good spatial resolution of the ECEI system.

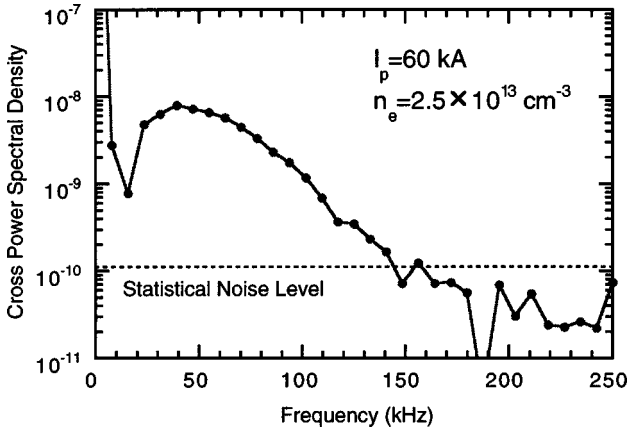

FIG. 6. Cross power spectral density of T_e fluctuations measured at 2.6 cm to the high field side of the magnetic axis and 6.5 cm below the tokamak midplane. The data are comprised of four similar Ohmic discharges with a total sampling length of one second at the flat top phases. The root-mean-square value of the relative T_e fluctuations is 2.1%.

from the ECRH interference. In ECRH discharges, this high pass filter limits the operation range of the ECEI system to above 113.6 GHz. In Ohmic discharges, it can be taken off to extend the operation frequency down to 100 GHz. The system is characterized in cases with and without this filter, and the difference in system performance is negligible. The only noticeable change is that the interchannel spacing decreases from 13 to 12.5 mm.

III. EXPERIMENTAL RESULTS

The ECEI system was installed on RTP in August 1997 and tested in both Ohmic and ECRH discharges. When operating at a LO frequency of 115 GHz, the rf to IF conversion loss of the middle channels is estimated to be about 13 dB. Using 3 dB N.F. IF amplifiers, this yields a system electronic noise temperature of 1 eV. This is about ten times smaller than that of the prototype ECEI system.[6] Due to less LO drive, the noise temperature of the edge channels may increase to 2 or 3 eV. With the setup shown in Fig. 3, the radiation noise would be 35 eV for a plasma with $T_e = 1$ keV.[5] Thus, the electronic noise is negligible.

The spatial resolution of the ECEI system is demonstrated in Fig. 5. The time traces of the signals are obtained during ECRH. They are calibrated against the T_e profiles measured by double pulse Thomson scattering in the same discharge and shifted arbitrarily according to the vertical position of the channels. An $m=2$ mode is observed to be localized at the sawtooth inversion radius ($r \sim 3.5$ cm), with a radial extent of less than 2 cm. This mode is very stable, which can survive the sawtooth crashes. The up–down symmetry of the mode verifies the accuracy of the channel positions measured with the setup described in Sec. II C.

Shown in Fig. 6 is the power spectral density of a broadband turbulent T_e fluctuation measured with ECEI in RTP. The rms value of the relative T_e fluctuation is 2.1%, which is smaller than the relative radiation noise of 3.5% (see above). Owing to the reduced interchannel crosstalk, a minimum detectible fluctuation level of 0.06% is achieved. The fact that this mode was first found in RTP about 7 cm above and below the tokamak midplane demonstrates the advantage of the ECEI system as a unique turbulence diagnostic. Extensive experiments are being carried out on RTP to measure the spatial distribution of the fluctuations, to investigate the characteristics and drive force of the turbulence, and to determine their contribution to anomalous transport.

ACKNOWLEDGMENTS

This work is supported by the U.S. Department of Energy under Contract Nos. DE-FG03-95ER-54295 and W-7405-ENG-48, and by NWO and EURATOM. One of the author (B.H.D.) wish to acknowledge Gary Potwin for useful suggestions in the electronics, C. Liang and J. Feng for their help in printed circuit board fabrication, H. Lu for the help in testing the electronics, and D. Smit for the help in system installation.

[1] A. E. Costley, R. J. Hastie, J. W. M. Paul, and J. Chamberlain, Phys. Rev. Lett. **33**, 758 (1994).
[2] N. J. Lopes Cardozo *et al.*, Phys. Rev. Lett. **73**, 256 (1994).
[3] N. J. Lopes Cardozo *et al.*, Plasma Phys. Controlled Fusion **39**, B303 (1997).
[4] J. W. Connor, Plasma Phys. Controlled Fusion **35**, B293 (1993).
[5] G. Cima, Phys. Plasmas **2**, 720 (1995).
[6] R. P. Hsia, B. H. Deng, W. R. Geck, C. Liang, C. W. Domier, N. C. Luhmann, Jr., D. L. Brower, and G. Cima, Rev. Sci. Instrum. **68**, 488 (1997).
[7] B. H. Deng, D. L. Brower, G. Cima, C. W. Domier, N. C. Luhmann, Jr., and C. Watts, Phys. Plasma. (submitted).
[8] C. C. Chen, IEEE Trans. Microwave Theory Tech. **21**, 1 (1973).